ACS APPLIED MATERIALS & INTERFACES

Research Article

www.acsami.org

High-Performance Small Molecule/Polymer Ternary Organic Solar Cells Based on a Layer-By-Layer Process

Weichao Chen,[†] Zhengkun Du,[†] Manjun Xiao,[†] Jidong Zhang,[‡] Chunpeng Yang,[†] Liangliang Han,[†] Xichang Bao,[†] and Renqiang Yang*[,†,§]

[†]CAS Key Laboratory of Bio-based Materials, Qingdao Institute of Bioenergy and Bioprocess Technology, Chinese Academy of Sciences, Qingdao 266101, China

[‡]State Key Laboratory of Polymer Physics and Chemistry, Changchun Institute of Applied Chemistry, Chinese Academy of Sciences, Changchun 130022, China

[§]State Key Laboratory of Luminescent Materials and Devices, South China University of Technology, Guangzhou 510641, China

Supporting Information

ABSTRACT: The layer-by-layer process method, which had been used to fabricate a bilayer or bulk heterojunction organic solar cell, was developed to fabricate highly efficient ternary blend solar cells in which small molecules and polymers act as two donors. The active layer could be formed by incorporating the small molecules into the polymer based active layer via a layer-by-layer method: the small molecules were first coated on the surface of poly(3,4-ethylenedioxy-thiophene):poly(styrenesulfonate) (PEDOT:PSS), and then the mixed solution of polymer and fullerene derivative was spin-coated on top of a small molecule layer. In this method, the small molecules in crystalline state were effectively mixed in the active layer. Without further optimization of the morphology of the ternary blend, a high power conversion efficiency (PCE) of 8.76% was obtained with large short-circuit current density (J_{sc}) (17.24 mA cm^{-2}) and fill factor (FF) (0.696). The high PCE resulted from not only enhanced light harvesting but also more balanced charge transport by incorporating small molecules.

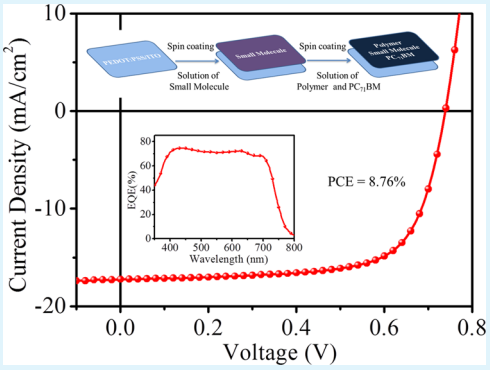

KEYWORDS: *ternary blend solar cells, layer-by-layer, small molecules, polymers, crystalline*

1. INTRODUCTION

Bulk heterojunction organic solar cells (OSCs) have become promising candidates for commercial solar energy conversion product owing to their low cost, light weight, mechanical flexibility, and approaching benchmark of industrial application.[1−8] Many efforts have been extensively investigated to improve the power conversion efficiency (PCE) of OSCs including the development of new narrow band gap conjugated materials with suitable energy levels,[9−15] interface engineering,[16−20] morphology control using processing additives or post-treatments,[21−24] and development of new device structures.[25−27] Recently, the PCE has exceeded 9% for binary single-junction OSCs based on devices with only small molecules or polymers as donors.[28−33]

Although the development of narrow band gap donor materials enhances the light absorption of binary blend OSCs, the narrow full width at half-maximum of absorption spectrum still hinders the utilization of the solar spectrum. An attractive strategy to overcome the spectral limitation of binary blend OSCs is to employ a ternary blend with the incorporation of additional component in binary blend OSCs.[27,34−38] Also, a third such component should exhibit the complementary absorption spectrum with the binary to extend the absorption of the solar spectrum and suitable energy level for exciton dissociation and charge carrier extraction.[39−42] Currently, the ternary blend OSCs based on polymer as the host donor have drawn much attention,[43−48] and the efficiency has exceeded 8% using polymer or small molecule as complementary donor.[36,40,49,50] In the ternary blend OSC, the morphology of the blend active layer is also one of critical parameters, which was similar to the binary blend OSC.[51−53] Nanoscale interpenetrating networks with appropriate phase-segregated domains and large interfacial area between donor and acceptor are important for achieving efficient exciton dissociation and favorable charge carrier transport.[54]

At present, the active layer of conventional ternary blend OSC is usually prepared by spin coating the mixed solution of three components directly. The incorporation of the third component makes the active layer of ternary blend OSC exhibit different film-forming characteristics as compared to those of the corresponding binary blend OSC. Also, much work has been done to control the nanoscale morphologies, such as

Received: July 31, 2015
Accepted: October 5, 2015
Published: October 5, 2015

DOI: 10.1021/acsami.5b07015
ACS Appl. Mater. Interfaces 2015, 7, 23190−23196

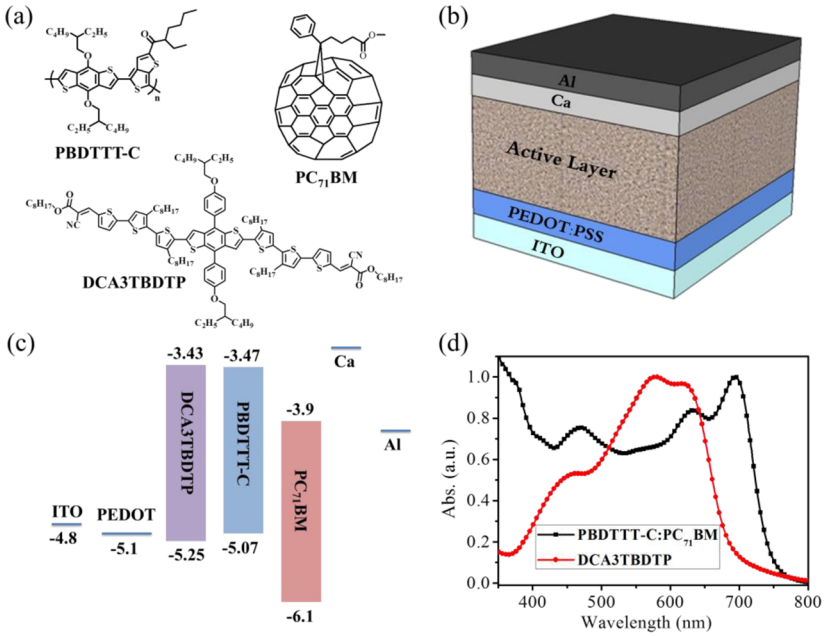

Figure 1. (a) Chemical structures of PBDTTT-C, DCA3TBDTP, and $PC_{71}BM$, (b) the device structure, (c) the energy levels of the materials, (d) the absorption spectra of the small molecule DCA3TBDTP and the polymer PBDTTT-C:$PC_{71}BM$ blend films.

employing a ternary solvent system (mixing the high-boiling solvent into the binary solvents) to obtain a fine nanostructure for high-performance ternary blend OSCs.[55] However, the film-forming process becomes more complex. In order to obtain high device performance in conventional ternary blend OSC, a lot of work is needed to further optimize the morphology and the ratio of three components. Therefore, it is necessary to develop a simple and effective method to prepare highly efficient ternary blend OSCs.

The layer-by-layer (LBL) solution-processed method has received much attention to prepare highly efficient organic solar cells.[56−59] Using this method, the bulk heterojunction OSC could be fabricated when solvents for the second layer could be diffused into the first layer, and if not, the planar heterojunction OSC could be fabricated. Highly efficient bulk heterojunction OSCs with PCE of 6.18% were fabricated by Zhan et al., and displayed appropriate vertical phase separation.[56] Zhan et al. also fabricated the highly efficient binary planar heterojunction OSC based novel small molecules with selective solubility as donor, which showed a high FF (0.75) benefit from the high mobility of small molecules.[57] In addition, this method had been used to prepare OSC with complex p-i-n-like structure (donor/donor:acceptor/acceptor).[58] Therefore, the layer-by-layer solution-processed method was simple and available for fabrication of highly efficient OSC. However, this method has not been used for fabrication of ternary blend OSC.

In this work, the LBL processed method was developed to fabricate efficient ternary blend OSCs based on polymer (PBDTTT-C) and small molecule (DCA3TBDTP) as donors, and $PC_{71}BM$ as acceptor. The chemical structures of materials are shown in Figure 1a, and the device structure is shown in Figure 1b. The pure small molecule DCA3TBDTP was first deposited on PEDOT:PSS by spin coating, and then the mixed solution (o-dichlorobenzene (o-DCB) was used for solvent) of polymer PBDTTT-C and $PC_{71}BM$ was spin-coated on top of the small molecule layer. In this case, although o-DCB could not dissolve the small molecules, the small molecular layer was broken into pieces due to the effect of o-DCB. Also, the small molecules in crystalline form were penetrated into the binary blend to form the active layer. A highly efficient ternary blend OSC with PCE of 8.76% was obtained without further optimizing the morphology of the active layer.

2. EXPERIMENTAL SECTION

Materials. Polymer PBDTTT-C was purchased from Solarmer, and $PC_{71}BM$ was obtained from American Dye Sources (ADS). The small molecule DCA3TBDTP was synthesized in our group. Patterned ITO glass with a sheet resistance of 15 Ω per square was obtained from Shenzhen Display (China). All of these materials were used as received without further purification.

Characterization. Atomic force microscopy (AFM) was employed to measure the morphologies of films by an Agilent 5400 with tapping mode. Transmission electron microscope (TEM) images were recorded on a Hitachi H-7650 transmission electron microscope at an accelerating voltage of 100 kV. Absorption spectra were measured with a Hitachi U-4100 UV−vis−NIR scanning spectrophotometer. The structure of the active layers was analyzed using X-ray diffraction (XRD), Bruker D8 ADVANCE.

Device Fabrication and Testing. The solar cells were prepared with the structure ITO/PEDOT:PSS/active layer/Ca/Al. Patterned ITO-coated glass was cleaned by ultrasonication in ITO detergent, deionized water, acetone, and isopropanol for 20 min each time, and then exposed to oxygen plasma for 6 min. PEDOT:PSS (Baytron P VP Al 4083) was deposited by spin coating onto ITO-coated glass substrates, and then annealed at 160 °C for 20 min. Subsequently, the substrate was transferred to a glovebox. The small molecule layer was prepared by spin coating the solution of pure DCA3TBDTP solution in chloroform onto PEDOT:PSS for 20 s, and then the complete active layer was prepared by spinning the mixed solution of polymer PBDTTT-C and $PC_{71}BM$ on the small molecule layer. The thickness of the small molecules was controlled by changing the spin speed from 600 to 3000 rpm. The weight ratio of PBDTTT-C:$PC_{71}BM$ was 1:1.5, and the total concentration was 31.25 mg/mL in o-dichlorobenzene (o-DCB). The spin speed and spin coating time for PBDTTT-C:$PC_{71}BM$ solution were about 1250 rpm and 60 s, respectively, and the resulting thickness was about 110 nm. Finally, after the samples were transferred to a vacuum chamber, Ca (10 nm) and Al (100 nm) were deposited via a mask to define the active area of 0.10 cm^2 in high vacuum. Current density−voltage (J−V) characteristics were recorded

DOI: 10.1021/acsami.5b07015
ACS Appl. Mater. Interfaces 2015, 7, 23190−23196

with a Keithley 2420 source measure unit under illumination of an AM1.5G solar Oriel simulator with an intensity of 100 mW cm^{-2}, which was calibrated by a standard silicon photodiode. External quantum efficiency (EQE) curves were measured by a Newport 2931-C coupled with the 300 W xenon lamp.

3. RESULTS AND DISCUSSION

The energy levels of the three components are important for exciton dissociation, charge transport, and collection in ternary blend OSC. The highest occupied molecular orbital (HOMO) energy level and lowest unoccupied molecular orbital (LUMO) of DCA3TBDTP and PBDTTT-C are −5.25, −5.07 eV, and −3.43, −3.47 eV (calculated from the optical band gap and HOMO), respectively, as shown in Figure 1c. The energy levels are suitable for the charge separation and transport. In addition, the complementary absorption spectra of the three components could improve the light harvesting and consequently short-circuit current density (J_{sc}). As shown in Figure 1d, the main absorption of the small molecule DCA3TBDTP ranges from 450 to 650 nm, where the PBDTTT-C:$PC_{71}BM$ blend film has relatively weak absorption. The three components show good complementary spectral characteristics. Therefore, the small molecule DCA3TBDTP is appropriate as an additional donor to improve the performance of polymer based ternary blend OSC.

The ternary blend solar cells based on layer-by-layer method (LBL ternary blend OSCs) were fabricated with the traditional structure of ITO/PEDOT:PSS/active layer/Ca/Al (Figure 1b). The diagrammatic sketch about the preparation process of the LBL ternary blend active layer is shown in Figure 2a. First, the small molecule is covered on the PEDOT:PSS/ITO substrate by spin coating. Next, the whole active layer is completed after spin coating the mixed solution of polymer and $PC_{71}BM$ on the surface of the small molecule.

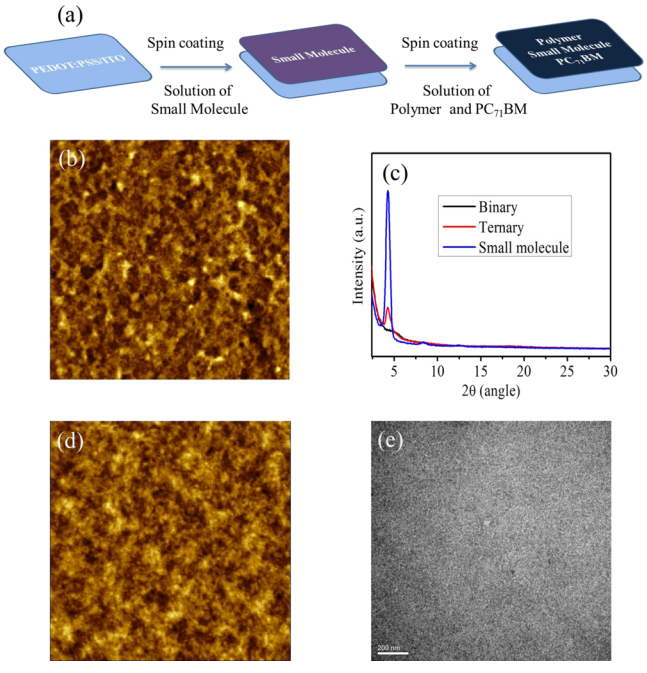

Figure 2. (a) Diagrammatic sketch about the preparation process of the active layer in LBL ternary blend OSC, (b) the bottom surface morphology (4 μm × 4 μm) of active layer in LBL ternary blend OSC, (c) the XRD curves of the active layers in binary and LBL ternary blend OSC and pure small molecular films, respectively, (d) the top surface morphology of the active layer in the LBL ternary blend OSC (4 μm × 4 μm), and (e) the TEM image of the active layer in the LBL ternary blend OSC.

The absorption spectra were examined to investigate the influence of the small molecule on the absorption of the active layer. As shown in Figure S1, the active layer showed broad and strong absorption from 350 to 750 nm. Compared with the binary blend layer, the LBL ternary blend layer exhibited higher absorption from 400 to 650 nm, which was contributed by the small molecule because it had strong absorption in this range as shown in Figure 1d. The absorption further confirmed that the small molecules could be incorporated into the active layer using this method. Meanwhile, the absorption intensity was increased gradually with increasing the thickness of small molecules. Thus, the ratio of small molecule in active layer could be tuned by changing its initial thickness, which can be employed to optimize the photovoltaic performance of the LBL ternary blend solar cells.

The scanning electron microscope (SEM) image of the cross section of the active layer was examined to investigate the change of the small molecular layer. As shown in Figure S2a, there are obvious PEDOT:PSS layer and the active layer, but no evident small molecule layer. The bottom surface morphologies of the active layers were examined by atomic force microscope (AFM) to further investigate the interface between the anode and the active layer. The active layers of both devices were inverse transfer printed onto a copper screen covered with carbon diaphragm by dissolving the water. As shown in Figure 2b, the LBL ternary blend OSC showed the similar surface image with the binary blend OSC (Figure S2b), and low root-mean-square (RMS) roughness value of ca. 1.30 nm. This implied that the small molecules had no influence on interface contact between active layer and anode. The aggregation state of the small molecule in the active layer was examined by X-ray diffraction (XRD). As shown in Figure 2c, the film of the LBL ternary blend showed an obvious diffraction peak at which the small molecule DCA3TBDTP film also showed an evident diffraction peak.[60] However, the peak was absent in the binary blend film based on polymer and $PC_{71}BM$. It indicated that the peak belonged to the small molecules, and therefore, the small molecules in the LBL ternary blend film were crystalline. On the basis of the analysis of the above details, it was assumed that the small molecular layer was broken into small crystals by the o-DCB solution and then diffused into the active layer.

The surface morphologies of the small molecule layer and the active layer were investigated and shown in Figure S2c,d, respectively. Although many holes appear in the small molecule layer, the complete active layer displays an integrated film without holes and shows a smooth surface with RMS roughness value about 2.0 nm. Also, interestingly, the top surface morphology was very similar to that of PBDTTT-C:$PC_{71}BM$ binary blend film as shown in Figure S2d. The addition of the small molecule using this method has no influence on the initial top surface morphology of the binary blend film, which is different from the conventional ternary blend solar cells prepared with mixed solution of three components.[38,45,49] In addition to the surface morphology, the interpenetrating network structure in the bulk is also very important, which affects the charge transport and collection. A transmission electron microscope (TEM) was employed to explore the microstructure inside the bulk. In LBL ternary blend OSC, the active layer presented obvious dark and light domains as shown

DOI: 10.1021/acsami.5b07015
ACS Appl. Mater. Interfaces 2015, 7, 23190−23196

in Figure 2e, which implies that the good interpenetrating network structure was formed using this method. Also, the dark and light domains were also similar to those of binary blend OSC (Figure S2e and Figure 2e). The interpenetrating network structure inside the bulk was not disturbed by the small molecules. Therefore, the active layer can be prepared easily by this method without further optimizing the morphology of the ternary blend OSC. Therefore, this is an efficient way to incorporate the small molecular crystals into the polymer based active layer.

The device performance of the LBL ternary blend OSCs based on LBL method was investigated by changing the thickness of the small molecule layer. The binary blend OSC based on PBDTTT-C:$PC_{71}BM$ used as a reference device gave a PCE of 6.61% with a V_{oc} of 0.71 V, a J_{sc} of 15.94 mA cm^{-2}, and a FF of 0.584. After incorporating the small molecules with different thickness into active layer, all the LBL ternary blend solar cells show better performance in the experimental range as shown in Figure S3 and Table S1. The optimal PCE of 8.76% was obtained with V_{oc} = 0.73 V, J_{sc} = 17.24 mA cm^{-2}, and FF = 0.696, respectively, at the thickness of small molecule layer about 50 nm. The typical current density−voltage (J−V) curves of binary and LBL ternary blend solar cells under AM 1.5G illumination at 100 mW cm^{-2} are shown in Figure 3a, and

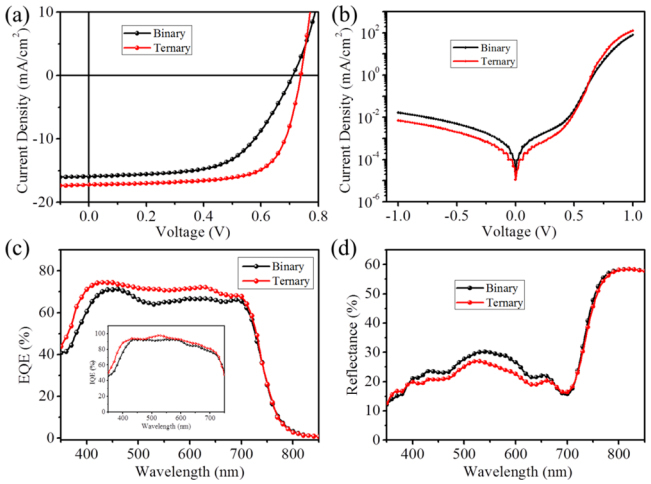

Figure 3. (a) Typical J−V curves of binary and LBL ternary blend solar cells under AM 1.5G illumination at 100 mW cm^{-2}, (b) the corresponding dark J−V curves, (c) EQE curves [inset: internal quantum efficiency (IQE)], and (d) reflectance spectra.

the corresponding parameters are summarized in Table 1. The incorporation of small molecules increased the J_{sc} of the LBL ternary blend OSC as expected. Also, the V_{oc} was a little higher than that of PBDTTT-C:$PC_{71}BM$ based binary cells and lower than that of DCA3TBDTP:$PC_{71}BM$ based cells (0.90 V) as shown in Figure S4. The higher V_{oc} may arise from the lower reverse saturation current as shown in Figure 3b. Interestingly, the FF was also enhanced significantly. All the device parameters were improved by incorporating the small molecule crystal into the active layer, indicating that the LBL processed method may be an effective way to fabricate the ternary blend solar cells.

The conventional ternary blend organic solar cells by blending three components in a single layer were also fabricated for comparison. The 7.46% PCE was obtained with J_{sc} of 16.96 mA/cm^2 and FF of 0.611 when adding 10% small molecules (w/w, small molecules/polymers) as shown in Figure S5 and Table S2, which is lower than our method. The morphologies of conventional ternary blend organic solar cells were investigated by AFM and TEM as shown in Figure S6. The surface displayed different morphology compared to the binary blend films and the LBL ternary blend films. Also, interpenetrating network structure in the bulk was also changed as seen in the TEM image. These indicated that the addition of small molecules in a conventional ternary device changed the morphology of binary blend films, and then influenced the device performance. The morphology optimization is crucial for fabricating high-performance ternary blend devices with a conventional method. Therefore, compared to the conventional method, our LBL method is relatively simple to fabricate ternary blend organic solar cells without further optimization of morphologies.

The photoelectric conversion process of LBL ternary blend OSC was investigated by employing the external quantum efficiency (EQE) curves and reflectance spectra of PBDTTT-C:$PC_{71}BM$ based OSCs before and after adding the small molecules. From Figure 3c, one can observe that the EQE curve of the optimal ternary blend OSC is higher than that of the binary blend one, especially in the wavelength range 450−650 nm, where the small molecules show strong absorption (Figure 1d). The high EQE probably results from the enhanced absorption of the active layer due to the good complementary absorption spectra of the small molecule and polymer. Meanwhile, the unreduced photoresponse of the polymer implies that the addition of small molecule does not hinder the photoelectric conversion process of polymer. The internal quantum efficiency (IQE), which was calculated from the measured effective absorption of the active layer (reflectance spectra, Figure 3d) and EQE, was employed to verify the contribution of the small molecules to the EQE enhancement. As shown in the inset of Figure 3c, the LBL ternary blend OSC exhibits high IQE (over 80% from 450 to 700 nm with peak value over 90%), which is a little higher than that of the binary blend solar cell. This means that the incorporation of small molecules has no negative influence on the exciton dissociation, and charge extraction, in reverse, enhances the process relatively. In other words, the excitons, which are generated from polymer, $PC_{71}BM$, and small molecule in the active layer, are separated to free charge carriers, and then the carriers could be collected at the electrodes. Therefore, the enhanced EQE can be mainly ascribed to increased effective light absorption of the active layer as shown in Figure 3d. The current density obtained by integrating the EQE curve with the standard solar

Table 1. Optimized Photovoltaic Parameters of the Binary and LBL Ternary Blend OSCs

solar cell	V_{oc} (V)	J_{sc} (mA cm^{-2})	FF	PCE (%)[a]	PCE_{max} (%)
binary	0.71(±0.005)	15.76 (±0.17)	0.576 (±0.08)	6.45(±0.19)	6.61
ternary	0.73(±0.005)	17.03 (±0.20)	0.688 (±0.09)	8.53(±0.21)	8.76

[a]The average PCE was obtained from over 10 devices.

DOI: 10.1021/acsami.5b07015
ACS Appl. Mater. Interfaces 2015, 7, 23190−23196

spectrum (AM 1.5G) is about 16.62 mA cm^{-2}, which is slightly smaller than the measured J_{sc} (17.24 mA cm^{-2}) with an error <5%.

The relation of photocurrent density (J_{ph}) versus effective voltage (V_{eff}) is further examined for LBL ternary and binary blend solar cells. The curve of J_{ph} versus V_{eff} is plotted in Figure 4a for the two devices: here, $J_{ph} = J_L - J_D$, where J_L and J_D stand

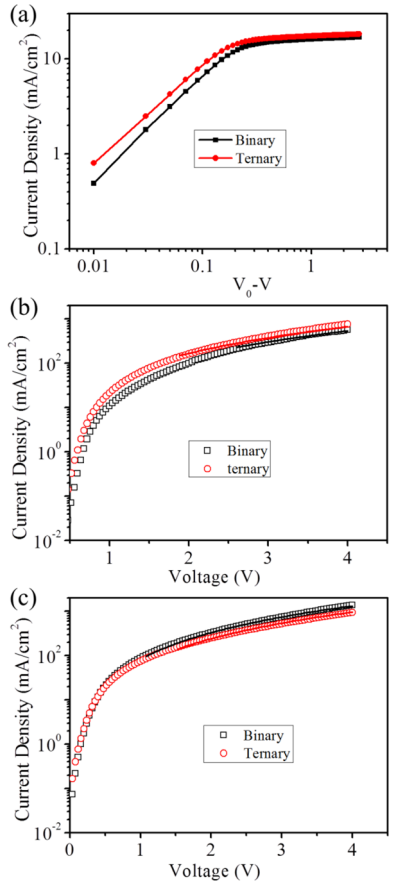

Figure 4. (a) Photocurrent density (J_{ph}) as a function of the effective voltage (V_{eff}) for the binary and LBL ternary blend OSCs under constant incident light intensity (AM 1.5G, 100 mW cm^{-2}), (b) $J-V$ characteristics of hole-only device in configuration of indium tin oxide (ITO)/PEDOT:PSS/active layer/Au, and (c) electron-only device in configuration of ITO/ZnO/active layer/Ca/Al in binary and LBL ternary blend OSC, respectively. The symbols are experimental data for the transport of holes and electrons, and the solid lines are fitted according to the space-charge-limited-current model.

for the current densities under AM 1.5G illumination and in the dark, respectively, and $V_{eff} = V_0 - V$, V_0 stands for the voltage at which $J_{ph} = 0$ and V is the applied voltage.[20,33] For both devices, the J_{ph} shows a linear dependence on the voltage at a low V_{eff} (<0.1 V), and is becoming saturated at a high V_{eff} (>1 V). It clearly shows that the LBL ternary blend OSC has a higher saturation photocurrent density (J_{sat}) than binary blend OSC, which means the LBL ternary blend OSC has a higher maximum exciton generation rate (G_{max}, given by $J_{sat} = eG_{max}L$, where L is the thickness of the photoactive layer, which reflects the maximum photons absorption) than that of the binary blend OSC. Therefore, the enhanced J_{sc} in LBL ternary blend OSC results from the enhanced light absorption and harvesting in the photoactive layer.

As shown in Table 1, FF was significantly increased from 0.584 to 0.696 when adding the small molecule, which was probably due to the enhanced charge carriers extracting properties in LBL ternary blend OSC. Hence, the charge carrier transport characteristics were investigated by single charge carrier devices with the space-charge-limited-current model,[61] which is described by the equation $J_{SCLC} = (9/8)\varepsilon_0\varepsilon_r\mu((V^2)/(L^3))$, where J is the current density, ε_0 is the dielectric constant of free space, ε_r is the relative permittivity of the transport medium, μ is the hole (μ_h) or electron (μ_e) mobility, V is applied voltage across the device, and L is the thickness of the active layer. As shown in Figure 4b,c, the LBL ternary blend solar cell exhibits relatively higher μ_h (2.41×10^{-4} cm^2 V^{-1} s^{-1}) but lower μ_e (3.48×10^{-4} cm^2 V^{-1} s^{-1}) compared to the binary blend solar cell ($\mu_h = 1.70 \times 10^{-4}$ cm^2 V^{-1} s^{-1}, $\mu_e = 4.38 \times 10^{-4}$ cm^2 V^{-1} s^{-1}). The crystalline small molecules usually have relatively high hole mobility. Therefore, the addition of small molecular crystalline material by the layer-by-layer method could improve the hole transport and increase the hole mobility of the active layer. The enhanced hole mobility yields a smaller ratio of the electron to hole mobility (μ_e/μ_h, 1.44 for ternary vs 2.58 for binary). Therefore, a more balanced charge transport was achieved by incorporation of the small molecule into the LBL ternary blend OSC. The more balanced charge transport could reduce space-charge effects, and then high FF is possible. Meanwhile, the high carrier mobility possibly also reduces the series resistance (R_s) of the devices. The LBL ternary blend OSC has a relatively lower R_s (3.7 Ω cm^2) than binary blend OSC (8.5 Ω cm^2). Therefore, the LBL ternary blend OSC showed higher FF than that of binary blend OSC.

4. CONCLUSION

In this work, a layer-by-layer solution-processed method was exploited to fabricate the ternary blend OSC using small molecules and polymers as donors. In this method, the small molecules can penetrate into the active layer of the ternary blend OSC, and exist in a crystalline state. A high-performance ternary blend OSC with PCE of 8.76% was obtained without further optimizing the morphologies of the active layers. Also, enhanced light harvesting and more balanced charge transport were realized in the solar cells. This work demonstrates a new direction of fabricating ternary blend OSCs with high PCE and a feasible route to improve performance of polymer solar cells.

■ ASSOCIATED CONTENT

Supporting Information

The Supporting Information is available free of charge on the ACS Publications website at DOI: 10.1021/acsami.5b07015.

High image of the top and bottom surface and TEM image of the active layer in the binary blend OSC, the bottom surface and SEM image of the cross section of active layer in the ternary blend OSC, the absorption spectra of the active layer in ternary blend OSC with different small molecule thickness, and the $J-V$ curves of the ternary blend OSC with different small molecule thickness (PDF)

■ AUTHOR INFORMATION

Corresponding Author

*E-mail: yangrq@qibebt.ac.cn.

DOI: 10.1021/acsami.5b07015
ACS Appl. Mater. Interfaces 2015, 7, 23190−23196

Author Contributions

The manuscript was written through contributions of all authors. All authors have given approval to the final version of the manuscript.

Notes

The authors declare no competing financial interest.

■ ACKNOWLEDGMENTS

This work was supported by the Ministry of Science and Technology of China (2014CB643501, 2010DFA52310), National Natural Science Foundation of China (61405209, 61107090, 51573205, 51503219, 51173199, 21274161).

■ REFERENCES

(1) Yu, G.; Gao, J.; Hummelen, J. C.; Wudl, F.; Heeger, A. J. Polymer Photovoltaic Cells - Enhanced Efficiencies via a Network of Internal Donor-Acceptor Heterojunctions. *Science* **1995**, *270*, 1789−1791.

(2) Gunes, S.; Neugebauer, H.; Sariciftci, N. S. Conjugated Polymer-based Organic Solar Cells. *Chem. Rev.* **2007**, *107*, 1324−1338.

(3) Li, G.; Zhu, R.; Yang, Y. Polymer Solar Cells. *Nat. Photonics* **2012**, *6*, 153−161.

(4) Thompson, B. C.; Frechet, J. M. J. Organic Photovoltaics - Polymer-fullerene Composite Solar Cells. *Angew. Chem., Int. Ed.* **2008**, *47*, 58−77.

(5) Chen, J. W.; Cao, Y. Development of Novel Conjugated Donor Polymers for High-Efficiency Bulk-Heterojunction Photovoltaic Devices. *Acc. Chem. Res.* **2009**, *42*, 1709−1718.

(6) Li, Y. F. Molecular Design of Photovoltaic Materials for Polymer Solar Cells: Toward Suitable Electronic Energy Levels and Broad Absorption. *Acc. Chem. Res.* **2012**, *45*, 723−733.

(7) Heeger, A. J. 25th Anniversary Article: Bulk Heterojunction Solar Cells: Understanding the Mechanism of Operation. *Adv. Mater.* **2014**, *26*, 10−28.

(8) Mazzio, K. A.; Luscombe, C. K. The Future of Organic Photovoltaics. *Chem. Soc. Rev.* **2015**, *44*, 78−90.

(9) Son, H. J.; Lu, L. Y.; Chen, W.; Xu, T.; Zheng, T. Y.; Carsten, B.; Strzalka, J.; Darling, S. B.; Chen, L. X.; Yu, L. P. Synthesis and Photovoltaic Effect in Dithieno 2,3-d:2 ′,3 ′-d ′ Benzo 1,2-b:4,5-b ′ dithiophene-Based Conjugated Polymers. *Adv. Mater.* **2013**, *25*, 838−843.

(10) Chu, T. Y.; Lu, J. P.; Beaupre, S.; Zhang, Y. G.; Pouliot, J. R.; Wakim, S.; Zhou, J. Y.; Leclerc, M.; Li, Z.; Ding, J. F.; Tao, Y. Bulk Heterojunction Solar Cells Using Thieno 3,4-c pyrrole-4,6-dione and Dithieno 3,2-b:2 ′,3 ′-d silole Copolymer with a Power Conversion Efficiency of 7.3%. *J. Am. Chem. Soc.* **2011**, *133*, 4250−4253.

(11) Huang, Y.; Guo, X.; Liu, F.; Huo, L. J.; Chen, Y. N.; Russell, T. P.; Han, C. C.; Li, Y. F.; Hou, J. H. Improving the Ordering and Photovoltaic Properties by Extending pi-Conjugated Area of Electron-Donating Units in Polymers with D-A Structure. *Adv. Mater.* **2012**, *24*, 3383−3389.

(12) Liang, Y. Y.; Yu, L. P. A New Class of Semiconducting Polymers for Bulk Heterojunction Solar Cells with Exceptionally High Performance. *Acc. Chem. Res.* **2010**, *43*, 1227−1236.

(13) Small, C. E.; Chen, S.; Subbiah, J.; Amb, C. M.; Tsang, S. W.; Lai, T. H.; Reynolds, J. R.; So, F. High-Efficiency Inverted Dithienogermole-Thienopyrrolodione-Based Polymer Solar Cells. *Nat. Photonics* **2012**, *6*, 115−120.

(14) Price, S. C.; Stuart, A. C.; Yang, L. Q.; Zhou, H. X.; You, W. Fluorine Substituted Conjugated Polymer of Medium Band Gap Yields 7% Efficiency in Polymer-Fullerene Solar Cells. *J. Am. Chem. Soc.* **2011**, *133*, 4625−4631.

(15) Cui, C.; Wong, W.; Li, Y. Improvement of Open-Circuit Voltage and Photovoltaic Properties of 2D-Conjugated Polymers by Alkylthio Substitution. *Energy Environ. Sci.* **2014**, *7*, 2276−2284.

(16) Kim, J. Y.; Kim, S. H.; Lee, H. H.; Lee, K.; Ma, W. L.; Gong, X.; Heeger, A. J. New Architecture for High-Efficiency Polymer Photovoltaic Cells Using Solution-Based Titanium Oxide as an Optical Spacer. *Adv. Mater.* **2006**, *18*, 572−576.

(17) Yuan, Y. B.; Reece, T. J.; Sharma, P.; Poddar, S.; Ducharme, S.; Gruverman, A.; Yang, Y.; Huang, J. S. Efficiency Enhancement in Organic Solar Cells with Ferroelectric Polymers. *Nat. Mater.* **2011**, *10*, 296−302.

(18) Steirer, K. X.; Ndione, P. F.; Widjonarko, N. E.; Lloyd, M. T.; Meyer, J.; Ratcliff, E. L.; Kahn, A.; Armstrong, N. R.; Curtis, C. J.; Ginley, D. S.; Berry, J. J.; Olson, D. C. Enhanced Efficiency in Plastic Solar Cells via Energy Matched Solution Processed NiOx Interlayers. *Adv. Energy Mater.* **2011**, *1*, 813−820.

(19) Seo, J. H.; Gutacker, A.; Sun, Y. M.; Wu, H. B.; Huang, F.; Cao, Y.; Scherf, U.; Heeger, A. J.; Bazan, G. C. Improved High-Efficiency Organic Solar Cells via Incorporation of a Conjugated Polyelectrolyte Interlayer. *J. Am. Chem. Soc.* **2011**, *133*, 8416−8419.

(20) He, Z. C.; Zhong, C. M.; Huang, X.; Wong, W. Y.; Wu, H. B.; Chen, L. W.; Su, S. J.; Cao, Y. Simultaneous Enhancement of Open-Circuit Voltage, Short-Circuit Current Density, and Fill Factor in Polymer Solar Cells. *Adv. Mater.* **2011**, *23*, 4636−4643.

(21) Peet, J.; Kim, J. Y.; Coates, N. E.; Ma, W. L.; Moses, D.; Heeger, A. J.; Bazan, G. C. Efficiency Enhancement in Low-Bandgap Polymer Solar Cells by Processing with Alkane Dithiols. *Nat. Mater.* **2007**, *6*, 497−500.

(22) Jo, J.; Kim, S. S.; Na, S. I.; Yu, B. K.; Kim, D. Y. Time-Dependent Morphology Evolution by Annealing Processes on Polymer:Fullerene Blend Solar Cells. *Adv. Funct. Mater.* **2009**, *19*, 866−874.

(23) Lee, J. K.; Ma, W. L.; Brabec, C. J.; Yuen, J.; Moon, J. S.; Kim, J. Y.; Lee, K.; Bazan, G. C.; Heeger, A. J. Processing Additives for Improved Efficiency from Bulk Heterojunction Solar Cells. *J. Am. Chem. Soc.* **2008**, *130*, 3619−3623.

(24) Liu, X. F.; Wen, W.; Bazan, G. C. Post-Deposition Treatment of an Arylated-Carbazole Conjugated Polymer for Solar Cell Fabrication. *Adv. Mater.* **2012**, *24*, 4505−4510.

(25) Kim, J. Y.; Lee, K.; Coates, N. E.; Moses, D.; Nguyen, T. Q.; Dante, M.; Heeger, A. J. Efficient Tandem Polymer Solar Cells Fabricated by All-Solution Processing. *Science* **2007**, *317*, 222−225.

(26) Chen, W. C.; Qiao, X. L.; Yang, J. B.; Yu, B.; Yan, D. H. Efficient Broad-Spectrum Parallel Tandem Organic Solar Cells Based on the Highly Crystalline Chloroaluminum Phthalocyanine Films as the Planar Layer. *Appl. Phys. Lett.* **2012**, *100*, 133302.

(27) Ameri, T.; Khoram, P.; Min, J.; Brabec, C. J. Organic Ternary Solar Cells: A Review. *Adv. Mater.* **2013**, *25*, 4245−4266.

(28) He, Z. C.; Zhong, C. M.; Su, S. J.; Xu, M.; Wu, H. B.; Cao, Y. Enhanced Power-Conversion Efficiency in Polymer Solar Cells Using an Inverted Device Structure. *Nat. Photonics* **2012**, *6*, 591−595.

(29) Ye, L.; Zhang, S. Q.; Zhao, W. C.; Yao, H. F.; Hou, J. H. Highly Efficient 2D-Conjugated Benzodithiophene-Based Photovoltaic Polymer with Linear Alkylthio Side Chain. *Chem. Mater.* **2014**, *26*, 3603−3605.

(30) Nguyen, T. L.; Choi, H.; Ko, S. J.; Uddin, M. A.; Walker, B.; Yum, S.; Jeong, J. E.; Yun, M. H.; Shin, T. J.; Hwang, S.; Kim, J. Y.; Woo, H. Y. Semi-Crystalline Photovoltaic Polymers with Efficiency Exceeding 9% in a Similar to 300 nm Thick Conventional Single-Cell Device. *Energy Environ. Sci.* **2014**, *7*, 3040−3051.

(31) Liao, S. H.; Jhuo, H. J.; Yeh, P. N.; Cheng, Y. S.; Li, Y. L.; Lee, Y. H.; Sharma, S.; Chen, S. A. Single Junction Inverted Polymer Solar Cell Reaching Power Conversion Efficiency 10.31% by Employing Dual-Doped Zinc Oxide Nano-Film as Cathode Interlayer. *Sci. Rep.* **2014**, *4*, 6813.

(32) Liu, Y.; Zhao, J.; Li, Z.; Mu, C.; Ma, W.; Hu, H.; Jiang, K.; Lin, H.; Ade, H.; Yan, H. Aggregation and Morphology Control Enables Multiple Cases of High-Efficiency Polymer Solar Cells. *Nat. Commun.* **2014**, *5*, 5293.

(33) Zhang, Q.; Kan, B.; Liu, F.; Long, G. K.; Wan, X. J.; Chen, X. Q.; Zuo, Y.; Ni, W.; Zhang, H. J.; Li, M. M.; Hu, Z. C.; Huang, F.; Cao, Y.; Liang, Z. Q.; Zhang, M. T.; Russell, T. P.; Chen, Y. S. Small-Molecule Solar Cells with Efficiency over 9%. *Nat. Photonics* **2015**, *9*, 35−41.

DOI: 10.1021/acsami.5b07015
ACS Appl. Mater. Interfaces 2015, 7, 23190−23196

(34) Chen, Y. C.; Hsu, C. Y.; Lin, R. Y. Y.; Ho, K. C.; Lin, J. T. Materials for the Active Layer of Organic Photovoltaics: Ternary Solar Cell Approach. *ChemSusChem* **2013**, *6*, 20−35.
(35) Ferenczi, T. A. M.; Muller, C.; Bradley, D. D. C.; Smith, P.; Nelson, J.; Stingelin, N. Organic Semiconductor: Insulator Polymer Ternary Blends for Photovoltaics. *Adv. Mater.* **2011**, *23*, 4093−4097.
(36) Yang, Y.; Chen, W.; Dou, L.; Chang, W.-H.; Duan, H.-S.; Bob, B.; Li, G.; Yang, Y. High-Performance Multiple-Donor Bulk Heterojunction Solar Cells. *Nat. Photonics* **2015**, *9*, 190−198.
(37) Khlyabich, P. P.; Rudenko, A. E.; Burkhart, B.; Thompson, B. C. Contrasting Performance of Donor−Acceptor Copolymer Pairs in Ternary Blend Solar Cells and Two-Acceptor Copolymers in Binary Blend Solar Cells. *ACS Appl. Mater. Interfaces* **2015**, *7*, 2322−2330.
(38) An, Q.; Zhang, F.; Li, L.; Wang, J.; Zhang, J.; Zhou, L.; Tang, W. Improved Efficiency of Bulk Heterojunction Polymer Solar Cells by Doping Low-Bandgap Small Molecules. *ACS Appl. Mater. Interfaces* **2014**, *6*, 6537−6544.
(39) Koppe, M.; Egelhaaf, H. J.; Dennler, G.; Scharber, M. C.; Brabec, C. J.; Schilinsky, P.; Hoth, C. N. Near IR Sensitization of Organic Bulk Heterojunction Solar Cells: Towards Optimization of the Spectral Response of Organic Solar Cells. *Adv. Funct. Mater.* **2010**, *20*, 338−346.
(40) Lu, L. Y.; Xu, T.; Chen, W.; Landry, E. S.; Yui, L. P. Ternary Blend Polymer Solar Cells with Enhanced Power Conversion Efficiency. *Nat. Photonics* **2014**, *8*, 716−722.
(41) Khlyabich, P. P.; Rudenko, A. E.; Street, R. A.; Thompson, B. C. Influence of Polymer Compatibility on the Open-Circuit Voltage in Ternary Blend Bulk Heterojunction Solar Cells. *ACS Appl. Mater. Interfaces* **2014**, *6*, 9913−9919.
(42) An, Q.; Zhang, F.; Li, L.; Wang, J.; Sun, Q.; Zhang, J.; Tang, W.; Deng, Z. Simultaneous Improvement in Short Circuit Current, Open Circuit Voltage, and Fill Factor of Polymer Solar Cells through Ternary Strategy. *ACS Appl. Mater. Interfaces* **2015**, *7*, 3691−3698.
(43) Gu, Y.; Wang, C.; Liu, F.; Chen, J. H.; Dyck, O. E.; Duscher, G.; Russell, T. P. Guided Crystallization of P3HT in Ternary Blend Solar Cell Based on P3HT:PCPDTBT:PCBM. *Energy Environ. Sci.* **2014**, *7*, 3782−3790.
(44) Khlyabich, P. P.; Burkhart, B.; Thompson, B. C. Compositional Dependence of the Open-Circuit Voltage in Ternary Blend Bulk Heterojunction Solar Cells Based on Two Donor Polymers. *J. Am. Chem. Soc.* **2012**, *134*, 9074−9077.
(45) Street, R. A.; Davies, D.; Khlyabich, P. P.; Burkhart, B.; Thompson, B. C. Origin of the Tunable Open-Circuit Voltage in Ternary Blend Bulk Heterojunction Organic Solar Cells. *J. Am. Chem. Soc.* **2013**, *135*, 986−989.
(46) Chi, C. Y.; Chen, M. C.; Liaw, D. J.; Wu, H. Y.; Huang, Y. C.; Tai, Y. A Bifunctional Copolymer Additive to Utilize Photoenergy Transfer and To Improve Hole Mobility for Organic Ternary Bulk-Heterojunction Solar Cell. *ACS Appl. Mater. Interfaces* **2014**, *6*, 12119−12125.
(47) Li, H.; Zhang, Z. G.; Li, Y. F.; Wang, J. Z. Tunable Open-Circuit Voltage in Ternary Organic Solar Cells. *Appl. Phys. Lett.* **2012**, *101*, 163302.
(48) Cheng, P.; Li, Y. F.; Zhan, X. W. Efficient Ternary Blend Polymer Solar Cells with Indene-C-60 Bisadduct as an Electron-Cascade Acceptor. *Energy Environ. Sci.* **2014**, *7*, 2005−2011.
(49) Zhang, Y.; Deng, D.; Lu, K.; Zhang, J.; Xia, B.; Zhao, Y.; Fang, J.; Wei, Z. Synergistic Effect of Polymer and Small Molecules for High-Performance Ternary Organic Solar Cells. *Adv. Mater.* **2015**, *27*, 1071−1076.
(50) Zhang, J.; Zhang, Y.; Fang, J.; Lu, K.; Wang, Z.; Ma, W.; Wei, Z. Conjugated Polymer−Small Molecule Alloy Leads to High Efficient Ternary Organic Solar Cells. *J. Am. Chem. Soc.* **2015**, *137*, 8176−8183.
(51) Machui, F.; Rathgeber, S.; Li, N.; Ameri, T.; Brabec, C. J. Influence of a Ternary Donor Material on the Morphology of a P3HT:PCBM Blend for Organic Photovoltaic Devices. *J. Mater. Chem.* **2012**, *22*, 15570−15577.
(52) Burke, K. B.; Belcher, W. J.; Thomsen, L.; Watts, B.; McNeill, C. R.; Ade, H.; Dastoor, P. C. Role of Solvent Trapping Effects in Determining the Structure and Morphology of Ternary Blend Organic Devices. *Macromolecules* **2009**, *42*, 3098−3103.
(53) Campoy-Quiles, M.; Kanai, Y.; El-Basaty, A.; Sakai, H.; Murata, H. Ternary Mixing: A Simple Mmethod to Tailor the Morphology of Organic Solar Cells. *Org. Electron.* **2009**, *10*, 1120−1132.
(54) Goubard, F.; Wantz, G. Ternary Blends for Polymer Bulk Heterojunction Solar Cells. *Polym. Int.* **2014**, *63*, 1362−1367.
(55) Peng, Z.; Xia, Y.; Gao, F.; Xiong, K.; Hu, Z.; James, D. I.; Chen, J.; Wang, E.; Hou, L. A Dual Ternary System for Highly Efficient ITO-free Inverted Polymer Solar Cells. *J. Mater. Chem. A* **2015**, *3*, 18365−18371.
(56) Cheng, P.; Hou, J. H.; Li, Y. F.; Zhan, X. W. Layer-by-Layer Solution-Processed Low-Bandgap Polymer-$PC_{61}BM$ Solar Cells with High Efficiency. *Adv. Energy Mater.* **2014**, *4*, 1301349.
(57) Lin, Y. Z.; Ma, L. C.; Li, Y. F.; Liu, Y. Q.; Zhu, D. B.; Zhan, X. W. Small-Molecule Solar Cells with Fill Factors up to 0.75 via a Layer-by-Layer Solution Process. *Adv. Energy Mater.* **2014**, *4*, 1300626.
(58) Li, H.; Wang, J. Z. Layer-By-Layer Processed High-Performance Polymer Solar Cells. *Appl. Phys. Lett.* **2012**, *101*, 263901.
(59) Ayzner, A. L.; Tassone, C. J.; Tolbert, S. H.; Schwartz, B. J. Reappraising the Need for Bulk Heterojunctions in Polymer-Fullerene Photovoltaics: The Role of Carrier Transport in All-Solution-Processed P3HT/PCBM Bilayer Solar Cells. *J. Phys. Chem. C* **2009**, *113*, 20050−20060.
(60) Du, Z.; Chen, W.; Qiu, M.; Chen, Y.; Wang, N.; Wang, T.; Sun, M.; Yu, D.; Yang, R. Utilizing Alkoxyphenyl Substituents for Side-Chain Engineering of Efficient Benzo 1,2-b:4,5-b′ Dithiophene-Based Small Molecule Organic Solar Cells. *Phys. Chem. Chem. Phys.* **2015**, *17*, 17391−17398.
(61) Mihailetchi, V. D.; Wildeman, J.; Blom, P. W. M. Space-Charge Limited Photocurrent. *Phys. Rev. Lett.* **2005**, *94*, 126602.

DOI: 10.1021/acsami.5b07015
ACS Appl. Mater. Interfaces 2015, 7, 23190−23196